

Hidden Pd Mott-insulator states in quasi-one-dimensional Br-bridged Pd/Ni mixed-metal complexes

Kaoru Iwano

Graduate University for Advanced Studies, Institute of Materials Structure Science, High Energy Accelerator Research Organization,
1-1 Oho, Tsukuba 305-0801, Japan

(Received 6 October 2003; published 7 January 2004)

Sample averaging combined with the density-matrix renormalization-group method is applied to an extended Peierls-Hubbard model that describes quasi-one-dimensional Br-bridged Pd/Ni mixed-metal complexes. The mixing ratio is changed rather freely, under the condition that the other system parameters reproduce an experimental charge-density-wave (CDW) gap when the Pd concentration is 100%. Special emphasis is placed on discrepancies from Hartree-Fock results: overall suppression of the CDW phase and its drastic conversion to a Mott insulator beyond a certain Ni concentration. This is interpreted as a realization of a Pd Mott-insulator state that is usually hidden under the stable CDW state. We also pay our attention to carrier-induced state conversion. We here assume that extra electrons and holes are created by light irradiation. Obtained results predict a large amount of Mott insulator to CDW reverse conversion, particularly in the phase-transition region.

DOI: 10.1103/PhysRevB.69.045104

PACS number(s): 71.27.+a, 71.30.+h, 71.38.-k, 78.20.-e

Quasi-one-dimensional Br-bridged mixed-metal (M ; $M = \text{Pd}$ or Ni) complexes have been attracting much interest these years, mainly from a viewpoint of direct and spatial confrontation of two basic interactions, namely, interelectron interaction and electron-lattice (el-l) interaction. In particular, the strongest concern is in the formation of Pd^{3+} states. This state, never seen in the ordinary halogen (X)-bridged homometal Pd complexes ($X = \text{Cl}$, Br , or I), was confirmed by IR and Raman spectroscopies,¹ magnetic-susceptibility measurement,^{2,3} and x-ray diffractions⁴ in $[\text{Ni}_{(1-x)}\text{Pd}_x\text{Br}(\text{chxn})_2]\text{Br}_2$, and also clarified theoretically.⁵ The main topic of this paper is that its formation can be regarded as an appearance of a hidden Mott-insulator phase of Pd.

In the homometal Pd systems, all the known compounds exhibit charge-density wave (CDW), in which a sequence of valencies, $\dots \text{Pd}^{2+}\text{Pd}^{4+}\text{Pd}^{2+}\text{Pd}^{4+}\dots$ in the chain direction, is realized with halogen sublattice dimerization.⁶ This makes a clear contrast to the fact that all the Ni compounds exhibit Mott-insulator states, namely, a monovalency of $3+$, and no dimerization.⁶ In both the compounds, the outermost electronic orbitals are d_{z^2} ($4d_{z^2}$ for Pd and $3d_{z^2}$ for Ni), z axis being parallel to the chain direction, and have finite transfer energies between the nearest neighbors via the halogen sites. The established consensus is that the difference between the two compounds originates mainly from the relative strength of the on-metal Coulombic repulsion, to the el-l interaction that is working between the electrons on the metal sites and the neighboring X^- s. Namely, the Ni systems are Mott insulators, due to rather large on-site repulsion energy U_{Ni} on the Ni sites, while the Pd systems are in the CDW states, due to smaller on-site repulsion energy U_{Pd} .^{7,8} However, theoretical calculations predict that even the Pd systems own a Mott-insulator phase as a metastable state.⁹ This is not so surprising if we recall the fact that the CDW states in the Pd compounds have much smaller optical gaps than those in Pt compounds.⁶ We hence expect that the former compounds are much closer to the CDW “Mott-

insulator” boundary and that it will be possible to demonstrate experimentally the multistability in the above meaning.

The inclusion of Ni sites into the Pd systems plays a role of stabilizing such a metastable Mott-insulator state. This is very natural, because a Ni site owns a large U_{Ni} and tends to suppress charge disproportionation and, subsequently, lattice displacements around it. In the first theoretical paper,⁵ it was actually confirmed that 50% of Ni inclusion was sufficient to drive a whole system into a Mott insulator, although the treatment was limited in the Hartree-Fock (HF) approximations. In the subsequent paper,¹⁰ it was suggested that the above claim survived, even considering the electron correlation effect beyond the HF approximation. However, a rather large phonon frequency and a high temperature were used, in order to converge quickly a quantum Monte Carlo simulation. As a result, the obtained result remained at a very qualitative level, and complete and detailed investigation, including accurate evaluation of the electron correlation and x dependency, was left for further studies.

In this paper, we apply the density-matrix renormalization-group (DMRG) method¹¹ to this electronic system. One of the purposes of this work is therefore very straightforward: accurate identification of the true ground states. In particular, we seek it for each Pd/Ni distribution, which is assumed to be spatially random, based on the fact that no order among Ni and Pd sites is found in x-ray diffractions.¹² In such a case, we expect that the distinction between the HF calculation and that by the DMRG method can be drastic in some samples, and it actually is.

As another purpose, we also investigate how states change when an extra electron or a hole is injected. This is motivated by the fact that the efficiency of carrier formations in the Ni systems, particularly the Br-bridged Ni system, is rather high.¹³ In fact, even the photoexcitation to the lowest absorption peak gives a substantial amount of photoconduction, and the photoconductivity almost monotonically increases when the excitation photon energy is increased. We are basically interested in the phase-transition region of x , because more delicate and, therefore, more sensitive-to-

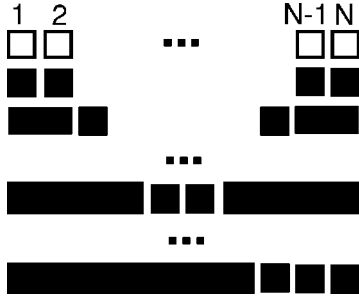


FIG. 1. Schematic picture of the first DMRG iteration. Open squares at the top mean the metal sites, and the closed squares and rectangles represent the blocks.

perturbation balancing seems to be existing there.

Following the preceding works,^{5,10} we make use of an extended Peierls-Hubbard model with a half-filled band:

$$H = - \sum_{l\sigma} t_0 (C_{l+1\sigma}^\dagger C_{l\sigma} + \text{H.c.}) + \sum_l \Delta_l n_l + \sum_l U_l n_{l\alpha} n_{l\beta} + V \sum_l n_l n_{l+1} - S \sum_l (Q_{l+1} - Q_l) n_l + \frac{S}{2} \sum_l Q_l^2, \quad (1)$$

where the creation and annihilation operators are related to the outermost d_{z^2} orbitals of Pd or Ni, and Q_l is the dimensionless displacement of the l th Br ion from each midpoint [see Fig. 2(a)]. The number operators, $n_{l\alpha}$ and $n_{l\beta}$, are those for the metal sites with spin up and down, respectively, and n_l means $n_{l\alpha} + n_{l\beta}$. Depending on the metal kind, the on-site Coulombic energy U_l and the site energy Δ_l take two values as $U_l = U_{Pd}$ or U_{Ni} and $\Delta_l = \Delta_{Pd}$ or Δ_{Ni} . In particular, the choice for U is motivated by the result by Okamoto *et al.*, who conclude that the U value for Ni is much larger than that for Pd.¹⁴ Meanwhile, the other parameters, namely, the electron transfer energy t_0 , the Coulombic energy between nearest-neighbor metal sites V , and the e-l interaction energy S are set to be constant. The biggest reason for this is that no reliable data for them are known yet, although this assumption is also based on the following physical consideration. Namely, these parameters are most sensitive to the M - M or M - X bond lengths, which are almost common for the Ni and Pd cases.⁶ We therefore expect no large differences in the parameter values between the two metal cases, and employ the above-mentioned approximation. We use the parameter values that were already employed in the first and second theoretical papers: $U_{Ni} = 5$ eV, $U_{Pd} = 1$ eV, and $t_0 = 1$ eV. As for the values of S and V , they should be chosen to reproduce CDW properties, because those parameters directly determine the stability of CDW. We here try two sets: $V = 0.5$ eV and $S = 0.2$ eV, and $V = 0.475$ eV and $S = 0.19$ eV. According to our exact-diagonalization calculation that is done in a 12-site ring, they give about 0.8 eV and 0.6 eV, respectively, as the peak energy of the lowest absorption band (see the insets in Fig. 3). Since the experimental value in $[\text{Pd}(\text{chxn})_2][\text{PdBr}_2(\text{chxn})_2]\text{Br}_4$ is around 0.7 eV,¹⁵ the above choices are regarded as reasonable. Lastly, we mention briefly the selection for Δ_l . The frequency of the ligand N-H stretching mode, which is traditionally a good

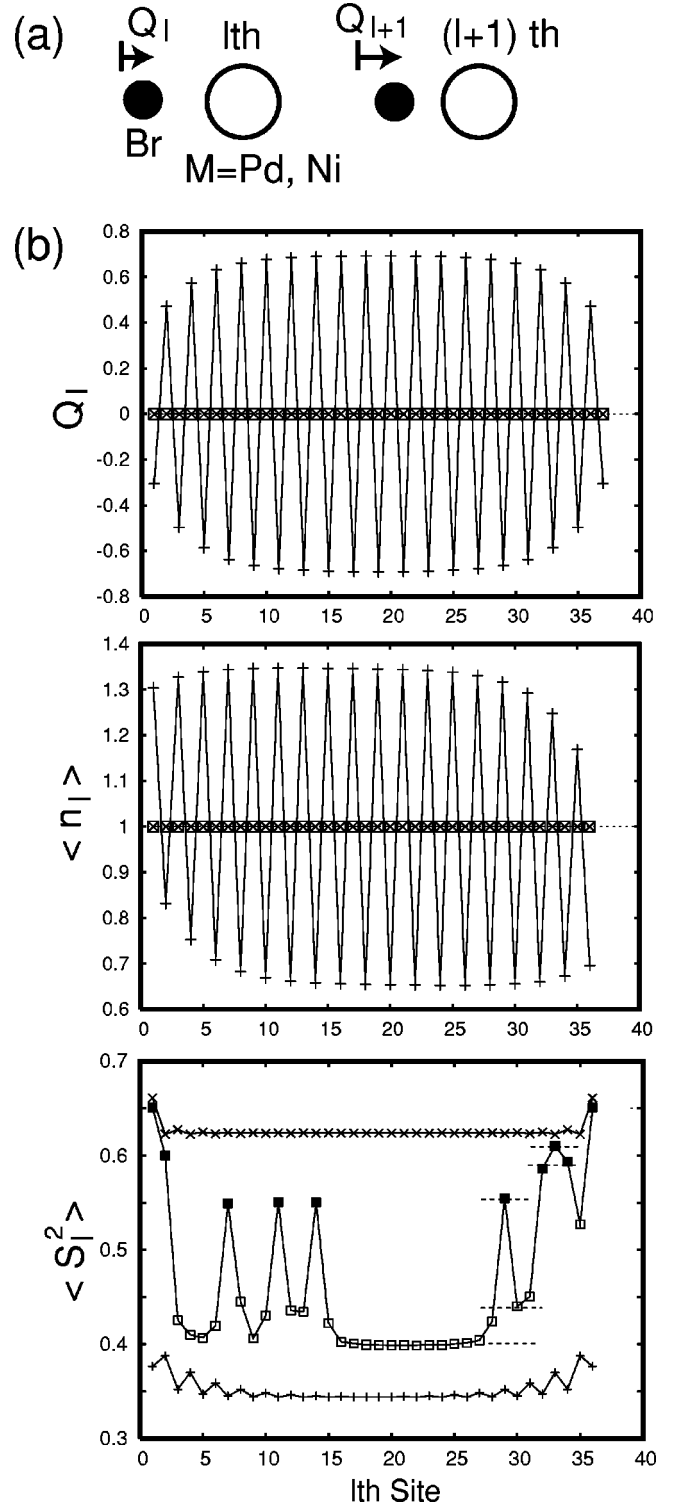


FIG. 2. (a) A segment of the mixed-metal MBr chain. (b) Quantities at $y=0$, 0.278, and 1, shown by “+,” squares, and “x,” respectively. For $y=0.278$, a typical sample is commonly used as an example, and the arrangement of Pd sites and Ni sites is specified in the bottom panel, by the closed squares (Ni sites) and the open squares (Pd sites).

marker of the valency of the surrounded metal ion, remains nearly the same value for Ni^{3+} , even when Pd ions are included.¹ This means almost negligible charge transfer be-

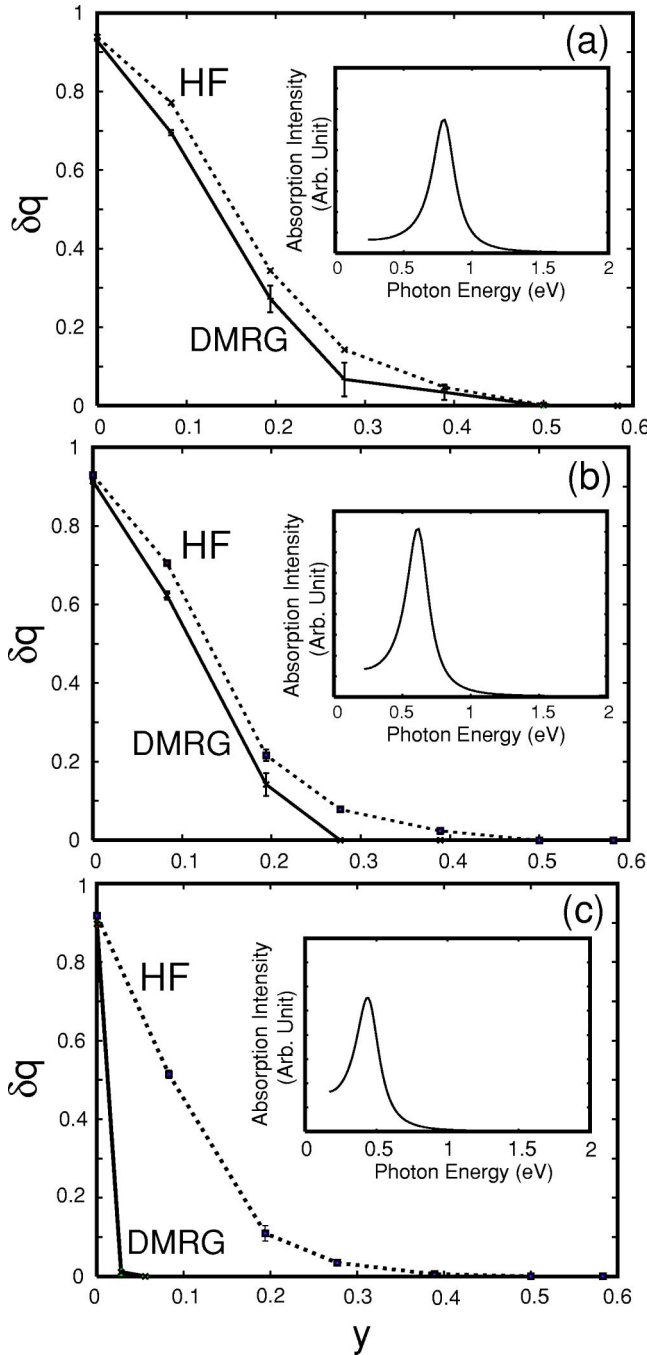


FIG. 3. Sample-averaged degrees of Br lattice displacements, as a function of y . (a) $S=0.2$ eV and $V=0.5$ eV. (b) $S=0.19$ eV and $V=0.475$ eV. (c) $S=0.18$ eV and $V=0.45$ eV. The other parameter values are common. Inset: the calculated absorption spectrum in a pure Pd chain.

tween them. We therefore impose a condition as $\Delta_{Ni} + (1/2)U_{Ni} + V = \Delta_{Pd} + (1/2)U_{Pd} + V$, to make the centers of gravity for the Ni and Pd bands coincide.

The ground states of the above Hamiltonian are obtained by the DMRG calculation. The size of the electronic system (the total number of metal sites), N , is 36, and the finite-system algorithm is used.¹¹ One special point is that the system is not uniform, having both the lattice displacements and

the random metal distribution. Consequently, we must always keep in mind the spatial positions of the blocks, and construct the blocks in the first iteration as depicted in Fig. 1. The lattice displacements are treated as classical, assuming an adiabatic situation, and optimized using an equilibrium condition, that is, $Q_l = \langle n_{l-1} \rangle - \langle n_l \rangle$. One Br site and two virtual metal sites are added at the ends: a system like v Br $M \cdots$ Br M Br v , where M is Pd or Ni, and “ v ” is a virtual metal site. These v states, of which the valencies are fixed at $3+$, play roles only in the lattice optimizations.

Convergence of the whole calculation is checked in the following way. First, the degree of state truncation (so called “ m ”) in the DMRG method is usually 100. We have also tried $m=150$ and confirmed that the result remains almost unchanged. The number of “iterations” in the same method is three. After three iterations, the ground-state energy differs from the previous one only by $\sim 1 \times 10^{-4}$ eV in mixed-metal cases, and much less in homometal cases. Second, we have also checked the convergence of the lattice optimization. As a general tendency, we find that the convergence is poorest for pure Pd cases. In the mixed-metal cases, on the other hand, high accuracy in energy, for example, $\sim 1 \times 10^{-4}$ eV, is more easily attained after 40 iterations. Lastly, it is emphasized that each optimization is done twice, started from two different initial conditions; one has zero displacements, while the other is of a staggered type with a large amplitude. The solution that gives the lower total energy is employed as a sample in averaging.

In Fig. 2(b), we show the lattice displacements and the expectation values of the local density n_l , and the local spin moments $S_l^2 \equiv S_{xl}^2 + S_{yl}^2 + S_{zl}^2$, for $y=0, 0.278$, and 1 . Here, the mixing ratio is defined as the concentration of Ni so that $y \equiv 1 - x$. For $y=0.278$, that is, ten Ni sites, a typical sample is selected for demonstration. As is most easily seen, $y=0$ gives staggered lattice displacements and charge densities, corresponding to the realization of a CDW. Meanwhile, we find zero displacements and uniform charge densities for $y=0.278$ and 1 , which are nothing but Mott-insulator states. In particular, the latter state should be called a modified Mott insulator, because the spin moments change from site to site, representing local metal arrangements (see the bottom panel). The largest change is of course due to whether it is a Ni site or a Pd site. Moreover we find, roughly speaking, three levels for each of the Ni and Pd spin moments, as are specified by the dashed horizontal lines. They correspond to three possibilities as Ni- M -Ni, Ni- M -Pd (Pd- M -Ni), and Pd- M -Pd, with M as the metal site that we focus on.

Next, we proceed to the sample-averaged results. In Figs. 3(a) and 3(b), which correspond to the real system, we show averaged degrees of Br lattice displacements, defined as $\delta q \equiv [1/(N+1)\sum_l \langle Q_l^2 \rangle]^{1/2}/Q_0$, where $\langle \cdots \rangle$ means the averaging over 96 samples, and Q_0 is the amplitude of the staggered displacements in each pure Pd case. The error bars, which are very small particularly in the HF calculations, are obtained by dividing the whole samples into four groups and calculating the standard deviation among the partial averages. Comparing the present DMRG results with those by the HF approximation, we notice the overall suppression in

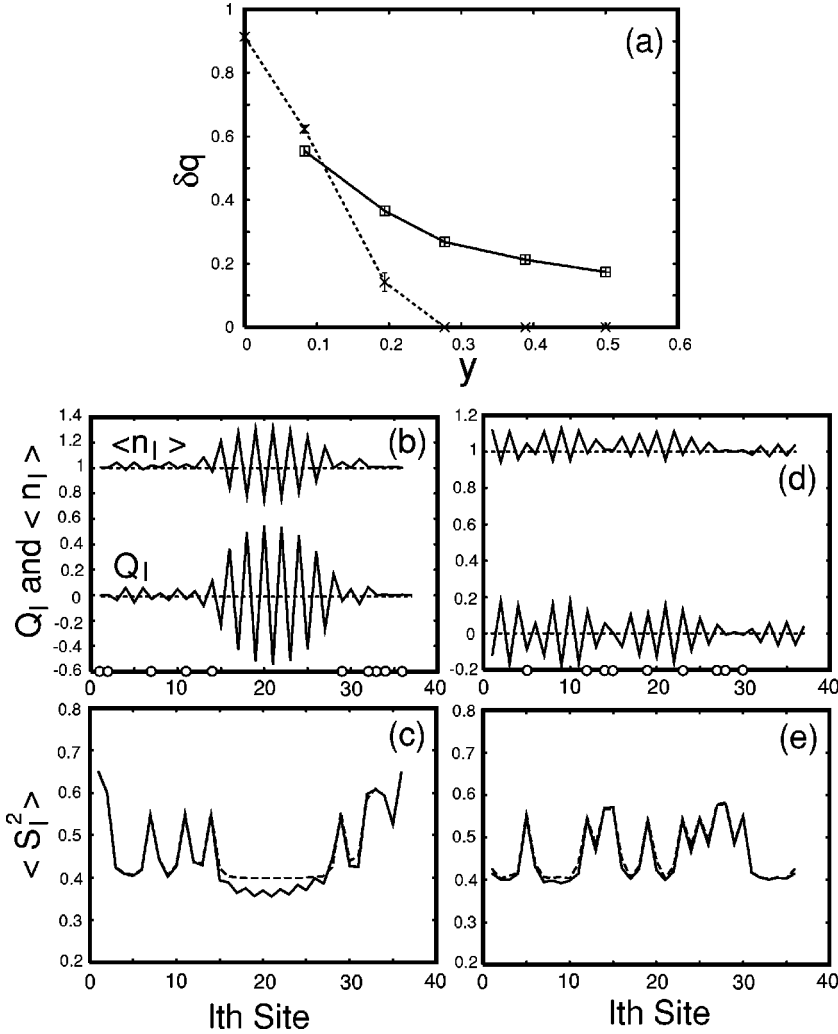


FIG. 4. (a) The degrees of lattice displacements in the presence of an extra electron. (b) and (c) show site-dependent quantities in the same sample as that in Fig. 2(b) ($y=0.278$). (d) and (e) show another sample with $y=0.278$. Quantities in the half-filled case and those after one-electron injection are shown by the dashed and solid lines, respectively. The open circles on the abscissas of (b) and (d) specify the Ni positions.

δq . Such a tendency is most conspicuous in the transition region around $y \sim 0.3$, and more enhanced in (b) because of the weaker couplings. Among all, the displacements seem to vanish completely at $y=0.278$ of (b), while those obtained by the HF approximation tend to survive up to higher Ni concentrations. We think that this stabilization of a Mott-insulator state originates from virtual magnon excitations associated with it, in the sense of a second-order perturbational theory.¹⁶ It is also emphasized that the discrepancy between the two curves can be regarded as qualitative, whose tendency is more clearly demonstrated in a weaker-coupling case, i.e., Fig. 3(c). Here, the CDW gap energy still remains finite as shown in the inset, while the Pd system itself is very close to the CDW “Mott-insulator” boundary. The above-mentioned discrepancy arises from the inaccurate boundary position determined by the HF approximation and the correct boundary position by the DMRG method. The averaged charge densities, normalized and subtracted from unity, give almost the same curves as those in Fig. 3, although they are not explicitly shown here. This originates both from the adiabatic approximation and from the fact that the surviving displacements and densities are synchronously staggered almost everywhere.

To compare the above results with the experimental ob-

servations, both the cases, i.e. (a) and (b), are consistent with the observations. Actually, the magnetic susceptibility and the IR measurement suggest that Pd^{3+} states are already realized after the inclusion of only 30% of Ni sites,^{1,2} which features are well reproduced in the present results.

As the last comment on Fig. 3, we discuss the finite-size effect. As plotted in Fig. 2(b), the lattice displacements in the CDW phase are suppressed on both the ends, being easily expected from the present boundary condition. The middle part, on the other hand, is almost flat and seems to give a bulk value (this is nothing but Q_0 in the definition of δq). According to the values δq at $y=0$ in Fig. 3, the displacements are reduced to about 90% of the bulk value, on the average. From this fact, we think that the other values in Fig. 3 will be also suppressed by 10% or so. We, however, emphasize that both the curves in each panel are obtained using the same boundary condition, and expect that the discrepancy between them will exist, being irrelevant to the finite-size effect.

In the rest, we argue carrier-induced effects. Since we assume that those carriers are formed as a result of photoexcitations, we start from the converged ground states in the half-filled systems and then add one carrier suddenly. In principle, the result is different depending on whether it is a hole

or an electron, because the new initial conditions destroy the electron-hole symmetry. However, our thorough investigation assures that the differences are practically very small, due to the almost staggered structures, and we only present the electron cases.

Figure 4(a) summarizes degrees of displacements at various y 's, with the solid (dashed) line as that after (before) the electron injection. The parameter values are the same as those for Fig. 3(b). As the first remark, the net direction of the induced change is different between low y 's and high y 's: δq decreases for the former and vice versa for the latter. It seems that $\delta q = 50\%$ in the original state is the border line, and it is natural because the two opposite directions cancel each other in such a situation. Next, focusing on the high y side, the maximum induced change, realized at $y \sim 0.3$, reaches as large as $+0.27$ in δq . Since this value is spatially averaged, it allows several interpretations. For example, if we assume that newly formed CDW domains have the almost same amplitude as that of the original CDW, Q_0 , the domain size should be about ten sites per totally 36 sites. A typical sample is depicted in (b) and (c), where a Ni-free zone located at the middle is transferred into a CDW domain. Since Q_0 in this case is about 0.69, this CDW domain has almost the same or slightly smaller amplitude. Meanwhile, we also find another type of samples. They show much smaller CDW amplitudes and, instead, larger domain sizes, as shown in (d) and (e). If we take account of such cases, the averaged CDW domain sizes can be interpreted as larger than the aforementioned value. Third, what is common to almost all the samples is that the induced changes occur at Pd sites or in Pd-rich regions, confirmed by the fact that S_I^2 show large changes at only Pd sites. Fourth, the new domains are formed in the following way. At first, the injected electron is trapped at the boundaries of a Ni-free zone. Then, the induced charge modulation triggers the lattice movements around it. Gradually, the density profile and the displacements grow into a CDW type. Last, we also comment on the quantum lattice effects, particularly the zero-point oscillations. From the frequency ($\omega \sim 200 \text{ cm}^{-1}$) of the M - X

stretching mode, a very rough calculation using $(1/2)\hbar\omega = (1/4)S\langle Q_I^2 \rangle$ gives about 0.25 for $\sqrt{\langle Q_I^2 \rangle}$. Comparing this value with the amplitude of the newly formed CDW domain in Fig. 3(b), it is likely that the order within the domain is actually destroyed. We think, however, that it will be possible to detect such domain formations through the detailed analysis of the photoinduced absorption spectra or electron spin resonance. Moreover, we also think that the aforementioned value for $\sqrt{\langle Q_I^2 \rangle}$ is rather exaggerated. Namely, in real systems the interchain interactions are not negligible and have a role of suppressing the quantum fluctuations. Although those interactions are not included in the present calculations, the adiabatic and single-chain treatment will be justified assuming that the effects from the other chains work as a kind of mean fields and augment the classical nature of the lattice.

To conclude, we have calculated the properties of Br-bridged Pd/Ni mixed-metal complexes at various mixing ratios, applying the DMRG method for the first time. A hidden state, that is, a Pd Mott-insulator state, manifests itself due to mixing effects. We find that the roles of electron correlation, namely, the discrepancy from the HF result, is always suppression of a CDW state and can be rather large at the transition region. We have also investigated the carrier-induced effects. The direction of the change is from CDW to Mott insulator at low Ni concentrations, while vice versa at high Ni concentrations. The largest change is found around $y \sim 0.3$. This means that one electron (one electron-hole pair) converts more than ten (twenty) Pd sites from a Mott-insulator domain to a CDW domain.

The author expresses his sincere gratitude for valuable experimental information by Professor S. Kuroda, Dr. K. Marumoto, Professor M. Yamashita, and Professor H. Okamoto. He is also thankful for fruitful discussions with Professor K. Nasu. This work was supported by the Grant-in-Aid (Grant No. 13640339) for Scientific Research from the Ministry of Education, Science, Sports and Culture of Japan. Lastly, he would like to thank the CPU time given from the computer center of KEK (SR8000 and PRIMEPOWER400).

¹M. Yamashita, T. Manabe, K. Inoue, T. Kawashima, H. Okamoto, H. Kitagawa, T. Mitani, K. Toriumi, H. Miyamae, and R. Ikeda, *Inorg. Chem.* **38**, 5124 (1999).

²K. Marumoto, H. Tanaka, S. Kuroda, T. Manabe, and M. Yamashita, *Phys. Rev. B* **60**, 7699 (1999).

³H. Tanaka, K. Marumoto, S. Kuroda, T. Manabe, and M. Yamashita, *J. Phys. Soc. Jpn.* **71**, 1370 (2002).

⁴Y. Wakabayashi, N. Wakabayashi, M. Yamashita, and T. Manabe, *J. Phys. Soc. Jpn.* **68**, 3948 (1999).

⁵K. Iwano, *J. Phys. Soc. Jpn.* **68**, 935 (1999).

⁶As an intensive review about the materials, H. Okamoto and M. Yamashita, *Bull. Chem. Soc. Jpn.* **71**, 2023 (1998).

⁷K. Nasu, *J. Phys. Soc. Jpn.* **52**, 3865 (1983).

⁸J.T. Gammel, A. Saxena, I. Batistic, A.R. Bishop, and S.R. Phillpot, *Phys. Rev. B* **45**, 6408 (1992).

⁹K. Iwano (unpublished).

¹⁰K. Iwano, *J. Phys. Soc. Jpn.* **71**, 174 (2002).

¹¹S.R. White, *Phys. Rev. B* **48**, 10 345 (1993).

¹²M. Yamashita (private communication).

¹³H. Okamoto, *J. Lumin.* **87-89**, 204 (2000).

¹⁴H. Okamoto, Y. Shimada, Y. Oka, A. Chainani, T. Takahashi, H. Kitagawa, T. Mitani, K. Toriumi, K. Inoue, T. Manabe, and Y. Yamashita, *Phys. Rev. B* **54**, 8438 (1996).

¹⁵H. Okamoto, K. Toriumi, T. Mitani, and M. Yamashita, *Phys. Rev. B* **42**, 10 381 (1990).

¹⁶K. Nasu, *J. Phys. Soc. Jpn.* **53**, 302 (1984).